

Self-modulation of cosmic rays in molecular clouds: Imprints in the radio observations

V. A. DOGIEL,¹ D. O. CHERNYSHOV,¹ A. V. IVLEV,² A. M. KISELEV,¹ AND A. V. KOPYEV¹

¹*I. E. Tamm Theoretical Physics Division of P. N. Lebedev Institute of Physics, 119991 Moscow, Russia*

²*Max-Planck-Institut für extraterrestrische Physik, 85748 Garching, Germany*

ABSTRACT

We analyze properties of non-thermal radio emission from the Central Molecular Zone (CMZ) and individual molecular clouds, and argue that the observed features can be interpreted in the framework of our recent theory of self-modulation of cosmic rays (CRs) penetrating dense molecular regions. For clouds with gas column densities of $\sim 10^{23}$ cm⁻², the theory predicts depletion of sub-GeV CR electrons, occurring due to self-modulation of CR protons and leading to harder synchrotron spectra in the sub-GHz range. The predicted imprints of electron depletion in the synchrotron spectra agree well with the spectral hardening seen in available radio observations of the CMZ. A similar, but even stronger effect on the synchrotron emission is predicted for individual (denser) CMZ clouds, such as the Sgr B2. However, the emission at frequencies above \sim GHz, where observational data are available, is completely dominated by the thermal component, and therefore new observations at lower frequencies are needed to verify the predictions.

Keywords: cosmic rays – turbulence – radio continuum: ISM – radiation mechanisms: non-thermal – Galaxy: center

1. INTRODUCTION

Ivlev et al. (2018) and Dogiel et al. (2018) developed a self-consistent model of cosmic ray (CR) interactions with molecular clouds, where CR penetration into the clouds is governed by the self-generated MHD turbulence. The resulting modulation of CR flux occurs in the diffuse envelopes around the clouds, before CRs penetrate into denser regions. Inside the dense regions MHD-fluctuations are damped by strong ion-neutral friction and particle propagate ballistically along the local magnetic field lines.

Both the CR spectrum and spectrum of the turbulence obey the excitation-damping balance, where the growth rate of magnetic fluctuations induced by CR flux in the envelope is compensated by damping of MHD waves due ion-neutral collisions (Ivlev et al. 2018). As a result, the CR spectrum inside the cloud develops a break at a certain energy $E_{\text{ex}}(N_{\text{H}_2})$, which is an increasing function of the cloud column density N_{H_2} (and whose value is determined by the shape of the interstellar spectrum). While the CR spectrum above E_{ex} remains unchanged, at lower energies the self-modulation leads to significant depletion of CR density, and can generate a universal

(i.e., independent of the interstellar spectrum) flux of CRs entering the clouds.

The CR depletion is expected to affect the gamma-ray emission due to proton-proton collisions, produced in dense molecular clouds of Central Molecular Zone (CMZ) as well as in molecular clouds in the vicinity of the Solar System (see de Boer et al. 2017; Dogiel et al. 2018; Tibaldo et al. 2021). Unfortunately, the value of E_{ex} turns out to be relatively small for the parameters of such clouds, typically varying between 0.3 – 3 GeV (Dogiel et al. 2018). As a result, the gamma-ray emission may only be affected at sub-GeV energies, where the resolution of Fermi-LAT becomes poor (Dogiel et al. 2018).

The MHD disturbances produced by dominant CR species, protons and nuclei, naturally also affect penetrating CR electrons. The main difference between electrons and hadrons of given energy is that electrons are able to produce gamma-ray emission at a higher energy, since bremsstrahlung photons take away a significant fraction of electron's energy. Therefore, if the electron bremsstrahlung was the dominant source of gamma-ray emission from a cloud, the effect of CR depletion would be seen at higher emission energies and, thus, would be likely detectable. Indeed, Yusef-Zadeh et al. (2013) pointed out that diffuse gamma-ray emission from the Galactic center at \sim GeV energies may be due to electron bremsstrahlung, as derived from a measured non-

thermal spectrum of radio emission (see Figure 12 of Yusef-Zadeh et al. 2013). On the other hand, it is generally believed that gamma-ray emission at such energies must be dominated by proton-proton collisions (see, e.g., Owen et al. 2021, and references therein).

This suggests that it may be difficult to find the effect of CR depletion in the gamma-ray range, and therefore it is worth shifting to lower emission energies. Indeed, features of the synchrotron emission from CR electrons modulated at \sim GeV energies should be observable at radio frequencies in \sim GHz range. Due to a very high resolution of radio telescopes, it is possible to observe individual clouds and, thus, to disentangle cloud emission from the background. The aim of this paper is to describe and quantify fingerprints of CR self-modulation that are expected in radio observations of molecular gas.

The paper is organized as follows. In Section 2 we discuss available radio observations from dense molecular clouds, in Section 3 we present a concise summary of the CR self-modulation theory and derive the expression for a modulated spectrum of CR electrons inside the clouds, in Section 4 we obtain the expected synchrotron emission from the CMZ and compare the theoretical results with observations, and in Section 5 we summarize our conclusions.

2. OBSERVED RADIO EMISSION FROM THE CMZ REGION AND FROM INDIVIDUAL MOLECULAR CLOUDS

One of the most promising targets for studies of the CR modulation is the CMZ – a region located near the Galactic center, with dimensions about $500 \text{ pc} \times 200 \text{ pc}$ in the Galactic plane and 30 pc in height (Ferrière et al. 2007). The gas is mostly concentrated in cold molecular clouds (see, e.g., Launhardt et al. 2002; Ferrière et al. 2007; Ginsburg et al. 2016; Mills et al. 2018) with the volume filling factor of $\sim 10\%$ and the average volume density of $\sim 10^4 \text{ cm}^{-3}$ (Mills 2017; Mills et al. 2018). The diffuse medium surrounding the clouds has an average gas density of $\lesssim 50 \text{ cm}^{-3}$ (Oka et al. 2005, 2019; Riquelme et al. 2018). Thus, the average column density of the CMZ, $N_{\text{H}_2}^{\text{CMZ}}$, is dominated by the contribution of dense clouds. Its value can be estimated as a product of the gas density averaged over the CMZ volume, $\sim 10^3 \text{ cm}^{-3}$, multiplied with the CMZ height, which yields $N_{\text{H}_2}^{\text{CMZ}} \sim 10^{23} \text{ cm}^{-2}$. The mean magnetic field strength in the Galactic center is estimated as $B \sim 0.1 \text{ mG}$ (Crocker et al. 2010), while in the clouds it can reach $B \sim 1 \text{ mG}$ (Ferrière 2009).

Yusef-Zadeh et al. (2013) found a strong spatial correlation between distributions of nonthermal radio sources and of molecular clouds in the CMZ, and concluded that the nonthermal radio continuum is produced by relativistic electrons. It was estimated that contribution of the thermal component into the total flux is less than 25%. The resulting spectral index of the integrated radio flux from the CMZ, defined as

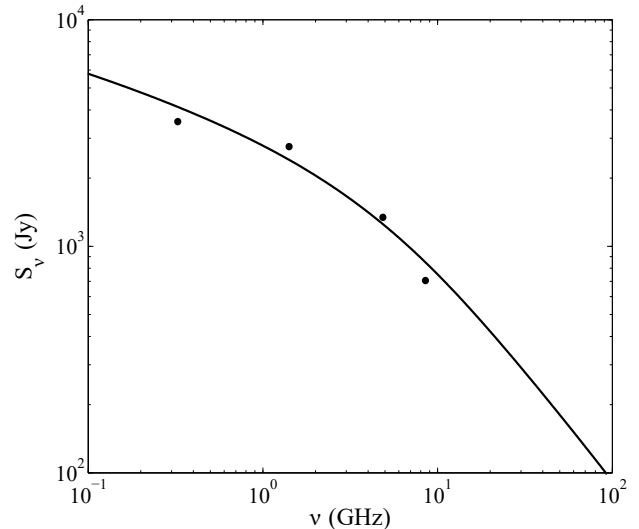


Figure 1. Diffuse non-thermal radio emission measured by Yusef-Zadeh et al. (2013) from the inner $2^\circ \times 1^\circ$ region around the Galactic center (bullets, statistical error bars are smaller than the symbols). The solid line shows the spectrum of synchrotron emission predicted by our model (see Section 4).

$\beta = -\Delta(\log S_\nu)/\Delta(\log \nu)$, is $\beta_{1.4 \text{ GHz}}^{325 \text{ MHz}} = 0.17 \pm 0.01$, $\beta_{4.5 \text{ GHz}}^{1.4 \text{ GHz}} = 0.58 \pm 0.01$, and $\beta_{8.5 \text{ GHz}}^{4.5 \text{ GHz}} = 1.14 \pm 0.01$. The measured spectrum S_ν is showed in Figure 1. These measurements can be naturally interpreted as a result of depletion of CR electrons in the CMZ, whose spectrum below the break is much harder than, e.g., in the Galactic local medium (see Bisschoff et al. 2019). The solid line shows the synchrotron spectrum predicted by our theoretical model, as described below in Section 4.

A stronger effect of CR depletion would be expected for very dense individual clouds. One of the suitable candidates is the giant molecular cloud complex Sgr B2 (e.g., Hüttemeister et al. 1995). While its average column density is about $N_{\text{H}_2}^{\text{CMZ}}$, in the central region of the Sgr B2 within $5 \text{ pc} \times 2.5 \text{ pc}$ we have $N_{\text{H}_2}^{\text{B2}} = 10^{24} - 10^{25} \text{ cm}^{-2}$ (Schmiedeke et al. 2016), i.e., 1–2 orders of magnitude higher than the average CMZ value.

Protheroe et al. (2008) (see also Jones et al. 2011; Meng et al. 2019) found that the radio emission from the central region of Sgr B2 is dominated by thermal emission of HII gas at frequencies above $\sim 0.3 \text{ GHz}$, as shown in Figure 2. Thus, unlike the CMZ, no indications of synchrotron-like emission from the Sgr B2 region were observed. We note that the same is true for several other very dense molecular clouds, located outside of the Galactic center: the complexes G333.125–0.562 and G333 (Jones et al. 2008) and IRAS15596 (Jones 2014). On the other hand, we point out that the radio spectra from the Sgr B2 region reported in Yusef-Zadeh et al. (2007, 2016) indicate a transition to non-thermal emission at the lowest observed frequencies of $\sim 0.3 \text{ GHz}$.

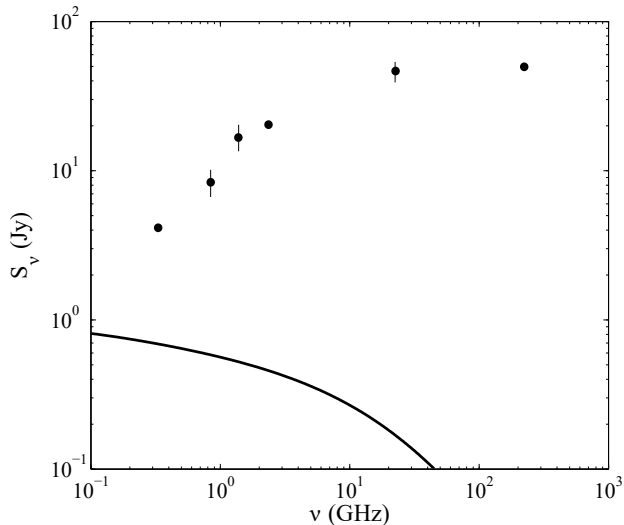


Figure 2. The spectrum of radio emission reported by Protheroe et al. (2008) from the central region of Sgr B2 (bullets). One can see a $S_\nu \propto \nu^2$ scaling at lower frequencies, indicating thermal nature of the emission. For comparison, we also plot the synchrotron emission spectrum (solid line) calculated for the central region of Sgr B2 from our model (see Section 4).

Below we are going to find out the values of parameters required for the radio emission from modulated spectrum of electrons to match the observations of the CMZ. We are also going to investigate the ratio between thermal and non-thermal emission components for individual molecular clouds, to determine the feasibility to detect the non-thermal component.

3. SPECTRUM OF CR ELECTRONS INSIDE DENSE CLOUDS

Ivlev et al. (2018) and Dogiel et al. (2018) developed the model of CR modulation in a diffuse envelope of a dense molecular cloud. It was assumed that energy losses in the envelope can be neglected and that the cloud absorbs a flux of CR protons¹ with a certain velocity u_p . For the proton spectrum $f_p(p)$ in the momentum space (normalized such that $\int f_p(p) dp$ is the total number density of CRs), this gives the boundary condition at the cloud edge in the following form:

$$S_p(p) = u_p f_p^{(c)}(p), \quad (1)$$

where $S_p(p)$ is the flux of CR protons into the cloud, p is their momentum and $f_p^{(c)}(p)$ is their spectrum at the cloud edge. The flux velocity u_p exceeds the Alfvén velocity v_A , which is a necessary condition of excitation of MHD waves by CRs. In the Appendix we calculate u_p for different propagation regimes in the cloud.

¹ For simplicity, here we only consider CR protons; heavier nuclei can be straightforwardly added, see Dogiel et al. (2018).

Given Equation (1), the flux of CR protons entering the cloud was estimated as (Dogiel et al. 2018)

$$S_p(p) = \frac{v_A f_p^{(0)}(p)}{1 - (1 - v_A/u_p) e^{-\eta_p(p)}}, \quad (2)$$

where $f_p^{(0)}(p)$ is the proton spectrum in the ISM, which is assumed to decrease with p faster than $\propto p^{-1}$. The “diffusion depth”,

$$\eta_p(p) = \int_0^{z_0} \frac{v_A dz}{D_p(z, p)}, \quad (3)$$

characterizes the relative importance of CR advection and diffusion in the envelope (Ivlev et al. 2018): diffusion determines the flux as long as $\eta_p \ll 1$, whereas for $\eta_p \gtrsim 1$ advection dominates and $S_p \approx v_A f_p^{(0)}$. The value of $\eta_p(p)$ depends on the proton diffusion coefficient $D_p(z, p)$, which is determined by the spectrum of self-generated turbulence. The integration limit $z_0(p)$ is the (momentum-dependent) outer border of the diffusion zone in the envelope (see Figure 2 of Ivlev et al. 2018).

If only a small fraction of penetrating protons is attenuated in a cloud, we can assume that their density in the cloud (where the self-generated turbulence is absent) remains almost constant. Therefore, Equations (1) and (2) allow us to estimate an average spectrum of any CR species inside the cloud, provided $D(z, p)$ is known.

Ivlev et al. (2018) obtained the expression for $\eta_p(p)$ assuming the excitation-damping balance for MHD waves, which is valid as long as $\eta_p \lesssim 1$. It was shown (Dogiel et al. 2018) that CR protons give the major contribution to the self-generated turbulence, while the contribution of other CR species can be largely ignored. The growth rate of MHD waves is proportional to the diffusion component of the flux (Ivlev et al. 2018), and hence the excitation-damping balance can be written as

$$\frac{\pi^2 e^2 v_A}{m_p c^2 \Omega} p \left[S_p(p) - v_A f_p^{(0)}(p) \right] = \nu, \quad (4)$$

where $\Omega = eB/(m_p c)$ is the proton gyrofrequency scale, B is the magnetic field strength, e is the elemental charge, m_p is the mass of the proton, and ν is the damping rate of MHD waves due to ion-neutral collisions. Using Equation (2), this can be solved for η_p , which yields

$$\eta_p(p) = \ln \left[\left(1 + \frac{\pi^2 e^2 v_A^2}{m_p c^2 \Omega \nu} p f_p^{(0)}(p) \right) \delta_p \right], \quad (5)$$

where $\delta_p = 1 - v_A/u_p > 0$. Since $\eta_p \geq 0$ by definition, the maximum momentum of modulated protons, p_{ex} , is determined from condition that the argument of the logarithm is equal to unity (see Dogiel et al. 2018). Only protons with $p < p_{\text{ex}}$ are able to resonantly excite MHD waves in the envelope (which leads to their

efficient scattering), while protons with larger momenta propagate through the envelope freely, without scattering.

Substituting Equation (5) into Equation (2) and assuming $\delta_p \approx 1$, one can estimate the average proton spectrum inside a cloud,

$$u_p f_p^{(c)}(p) \propto \begin{cases} p^{-1}, & \text{if } p_A \leq p \leq p_{\text{ex}}, \\ f_p^{(0)}(p), & \text{if } p \geq p_{\text{ex}}. \end{cases} \quad (6)$$

In the Appendix we demonstrate that u_p does not practically depend on p . Therefore, the spectrum has a universal form $f_p^{(c)}(p) \propto p^{-1}$ for $p_A \leq p \leq p_{\text{ex}}$, with p_A estimated from the condition $\eta_p(p_A) \sim 1$. We note that the universal dependence $S_p(p) \propto p^{-1}$, occurring for $0 < \eta_p \lesssim 1$ (where S_p is dominated by diffusion), follows directly from the excitation-damping balance, Equation (4). For $p \lesssim p_A$, where η_p exceeds unity and according to Equation (2) the proton flux converges to the advection component $v_A f_p^{(0)}(p)$, we again obtain $f_p^{(c)}(p) \propto f_p^{(0)}(p)$.

Now we can estimate the electron spectrum inside the cloud. Indeed, the diffusion coefficient for both protons and electrons is calculated as

$$D(p) \approx \frac{vB^2}{6\pi^2 k^2 W(k)}, \quad (7)$$

where $v(p)$ is the particle velocity, $k(p) = eB/(pc)$ is the resonant wavenumber, and $kW(k)$ is the total energy density of the proton-generated turbulence per unit $\log k$ range (i.e., $8\pi kW(k)/B^2$ is the dimensionless energy density). Therefore, the electron flux $S_e(p)$ is described by Equation (2) where the proton interstellar spectrum and the flux velocity are replaced with the respective electron values, $f_e^{(0)}$ and u_e , while the electron diffusion depth is

$$\eta_e(p) = \eta_p(p) \frac{v_p(p)}{v_e(p)}, \quad (8)$$

as follows from Equation (3). Assuming for simplicity that both electrons and protons are relativistic, $p \gg m_p c$, and setting $\delta_e \approx 1$, we obtain the electron spectrum inside the cloud,

$$u_e f_e^{(c)}(p) \propto \begin{cases} p^{-1} \frac{f_e^{(0)}(p)}{f_p^{(0)}(p)}, & \text{if } p_A \leq p \leq p_{\text{ex}}, \\ f_e^{(0)}(p), & \text{if } p \geq p_{\text{ex}}, \end{cases} \quad (9)$$

with the same p_A and p_{ex} as in Equation (6). For relativistic CRs, their interstellar spectra are well described by power-law dependencies, $f_{p,e}^{(0)}(p) \propto p^{-\gamma_{p,e}}$, with $\gamma_p \approx 2.7$ and $\gamma_e \approx 3.2$ (see e.g. [Bisschoff et al. 2019](#)). Thus, the electron spectrum inside a cloud scales as $f_e^{(c)}(p) \propto p^{-1+\gamma_p-\gamma_e} \approx p^{-1.5}$ (again, for $u_e = \text{const}$) within the ‘‘universal’’ momentum range of $p_A \leq p \leq p_{\text{ex}}$.

4. EXPECTED RADIO SPECTRUM FROM DENSE CLOUDS

Using the results of previous section as well as the expressions for u_p and u_e presented in the Appendix, we evaluate the electron spectrum $f_e^{(c)}(p)$ inside the cloud. This allows us to compute the total synchrotron emissivity \mathcal{P}_ν of ultra-relativistic electrons per unit volume ([Ginzburg & Syrovatskii 1965](#)),

$$\mathcal{P}_\nu \approx \frac{\sqrt{3}e^3 B_\perp}{m_e c^2} \int dp f_e^{(c)}(p) \frac{\nu}{\nu_*} \int_{\nu/\nu_*}^{\infty} dx K_{5/3}(x), \quad (10)$$

where $K_\alpha(x)$ is the McDonald function and

$$\nu_*(p) = \frac{3eB_\perp}{4\pi m_e c} \left(\frac{p}{m_e c} \right)^2, \quad (11)$$

is determined by the plane-of-the-sky magnetic field strength B_\perp . The emissivity scales as $\mathcal{P}_\nu \propto B^{(\gamma+1)/2} \nu^{-(\gamma-1)/2}$ for a power-law electron spectrum $f_e^{(c)}(p) \propto p^{-\gamma}$, with the contribution of individual electrons peaked at a frequency of $\nu(p) \approx 0.3\nu_*(p)$ ([Ginzburg & Syrovatskii 1965](#)). This indicates that (i) the synchrotron emission is primarily generated in denser regions, where the magnetic field is stronger, and (ii) the emission spectrum exhibits a break due to CR modulation. According to Equation (9), at higher frequencies, corresponding to unmodulated electrons with $p \gtrsim p_{\text{ex}}$, the emission varies as $\mathcal{P}_\nu \propto \nu^{-(\gamma_e-1)/2} \approx \nu^{-1.1}$, while at lower frequencies the spectrum becomes harder, $\mathcal{P}_\nu \propto \nu^{-(\gamma_e-\gamma_p)/2} \approx \nu^{-0.25}$.

For a quantitative comparison with available observations from the CMZ ([Yusef-Zadeh et al. 2013](#)), we assumed $n_{\text{H}_2} = 50 \text{ cm}^{-3}$ for the density of molecular hydrogen in the diffuse envelope, $B = 0.1 \text{ mG}$ for the average magnetic field (we note that this value does not practically affect the resulting radio spectrum), and used the solar abundance of carbon ions to calculate the Alfvén velocity and the ion-neutral damping in the envelope. The cloud column density, which determines the value of p_{ex} , was set to $N_{\text{H}_2}^{\text{CMZ}} = 10^{23} \text{ cm}^{-2}$. For the proton or electron spectra outside the envelope we used the model form suggested in [Ivlev et al. \(2015\)](#),

$$f_{e,p}^{(0)}(p) = \text{const} \frac{E^\alpha}{(E_0 + E)^\beta}, \quad (12)$$

where $E(p)$ is the proton or electron kinetic energy, $E_0 = 500 \text{ MeV}$ (same for both species), $\alpha = -0.8$ (-1.5) and $\beta = 1.9$ (1.7) for protons (electrons). These values of E_0 , α , and β were selected in [Ivlev et al. \(2015\)](#) to provide the upper bound for the available observational data on the CR ionization rate in diffuse gas ([Indriolo & McCall 2012](#)). Constant factors were chosen to ensure that the spectrum of relativistic protons is the same as in the local interstellar medium ([Acero et al. 2016](#)),

while the electron interstellar spectrum was enhanced by a factor of 10. The synchrotron emission flux was calculated by assuming that the radiation mainly comes from dense regions occupying $\sim 10\%$ of the total CMZ volume, $V_{\text{rad}} \sim 0.1V_{\text{CMZ}} \sim 10^{61} \text{ cm}^3$. The magnetic field in the dense regions was set 5 times stronger than the average field, $B_{\text{dense}} = 0.5 \text{ mG}$. The total emission flux at a distance $R_{\text{CMZ}} \approx 8 \text{ kpc}$ is then obtained as $S_\nu = P_\nu V_{\text{rad}} / (4\pi R_{\text{CMZ}}^2)$.

Furthermore, to explore the role of CR absorption in dense clouds, we considered a model case of the central region of Sgr B2, corresponding to the observations reported by Protheroe et al. (2008). In this case, we set the cloud column density to $N_{\text{H}_2}^{\text{B2}} = 10^{24} \text{ cm}^{-2}$, keeping the other parameters unchanged.

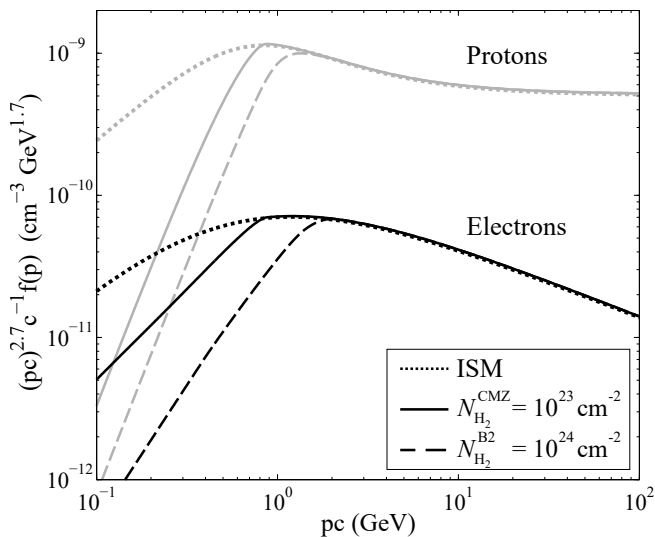


Figure 3. Modulated spectra of CR electrons and protons inside CMZ clouds. The solid lines represents the spectra inside an average CMZ cloud with the column density of $N_{\text{H}_2}^{\text{CMZ}} = 10^{23} \text{ cm}^{-2}$, the dashed lines correspond to the central region of Sgr B2 with $N_{\text{H}_2}^{\text{B2}} = 10^{24} \text{ cm}^{-2}$. For comparison, the dotted lines show the interstellar (unmodulated) spectra. For the shown energy range, the densities of secondary electrons (not displayed) are negligible compared to the respective modulated electron densities.

Figure 3 shows the results of our calculations, displaying self-modulated spectra of CR protons (grey lines) and the resulting modulated electron spectra (black lines). We see that the modulation for an average CMZ cloud (solid lines) leads to a depletion of sub-GeV electrons, but the depletion magnitude is less than a factor of ~ 3 for $pc \gtrsim 0.2 \text{ GeV}$. For the above parameters, this modulated energy range approximately corresponds to the frequency range between $\sim 0.3 \text{ GHz}$ and $\sim 3 \text{ GHz}$, i.e., up to the spectral break seen in the radio data depicted by the bullets in Figure 1. Therefore, the solid line in Figure 1, representing the calculated synchrotron

flux, provides a good agreement with the data, both in terms of the position of the spectral break and the slopes above and below the break.

The depletion of CR electrons in denser clouds, such as the central region of Sgr B2, starts at higher energies, as shown in Figure 3 by the dashed line. The depletion magnitude in this case is up to a factor of ~ 20 (for the same energy range). The corresponding synchrotron flux, plotted by the solid line in Figure 2, is too low to compete with the thermal emission. Note that the secondary electrons were estimated to have a negligible ($\lesssim 10\%$) contribution to the above results.

We point out that the predicted modulation of CR electrons can also be reflected in the continuum gamma-ray emission. A complete sky survey of the gamma-ray emission below 100 MeV was performed by COMPTEL imaging telescope (Schönfelder et al. 1993). The spectrum was analyzed by Strong et al. (1996), who concluded that the bremsstrahlung radiation in this range must be primarily produced by Galactic CR electrons. Therefore, the emission may indeed be affected by the electron depletion, but the spatial and energy resolution of the COMPTEL data is too poor to observe the effect. The spectral break is expected at around $0.1 - 0.3 \text{ GeV}$, both for proton- and electron-generated emission, and thus next-generation gamma-ray telescopes operating in this energy range, such as AMEGO (McEnery et al. 2019) and e-ASTROGAM (De Angelis et al. 2021), may be able to observe the depletion effect. The necessary condition for that would be their ability to resolve individual molecular clouds. In case of the CMZ, the required spatial resolution is about 1° .

5. CONCLUSIONS

We analyzed non-thermal radio emission from dense CMZ regions, and demonstrated that the observed spectral features can well be interpreted in the framework of our recent theory of CR self-modulation in molecular clouds (Ivlev et al. 2018; Dogiel et al. 2018). Our conclusions are summarized as following:

- Self-modulation of CR protons with energies below a certain threshold E_{ex} , determined by the column density of a cloud, generates a universal ($\propto E^{-1}$) flux of protons entering the cloud. This leads to a significant depletion of both the proton and electron densities below E_{ex} . Proton-proton collisions are generally believed to be the main source of gamma-ray emission from clouds. However, due to low spatial and energy resolutions of Fermi-LAT at the relevant sub-GeV energies, the effect of proton depletion cannot be observed (although next-generation gamma-ray telescopes may potentially be able to resolve the emission). On the other hand, thanks to a high resolution of radio telescopes in the $\sim \text{GHz}$ range, it is possible to

observe individual clouds and, thus, to detect the synchrotron emission of modulated electrons;

- Assuming power-law spectra of relativistic interstellar protons and electrons, with the respective spectral indices γ_p and γ_e , the electron (momentum) spectrum inside a cloud scales as $f_e(p) \propto p^{-1+\gamma_p-\gamma_e}$ for $p < p_{\text{ex}}$ and $f_e(p) \propto p^{-\gamma_e}$ for $p > p_{\text{ex}}$. This break naturally leads to a spectral break in the synchrotron emission;
- The radio continuum from the CMZ is evidently non-thermal (see Yusef-Zadeh et al. 2013) and, due to its large average column density of $N_{\text{H}_2}^{\text{CMZ}} \sim 10^{23} \text{ cm}^{-2}$, the CMZ is one of the most promising targets for studying the CR self-modulation. The value of $E_{\text{ex}}(N_{\text{H}_2}^{\text{CMZ}}) \sim 1 \text{ GeV}$ ensures the synchrotron spectral break at $\sim 1 \text{ GHz}$;
- The observed radio spectrum from the CMZ can be approximated by a double power-law dependence with $S_\nu(\nu) \propto \nu^{-0.17}$ below $\sim 1 \text{ GHz}$ and $S_\nu(\nu) \propto \nu^{-1.14}$ above $\sim 1 \text{ GHz}$ (see Figure 1). We demonstrate that this spectrum is well described

by our theory of CR self-modulation, assuming the interstellar proton and electron spectra in the CMZ have the shape of the local CR spectra, with the electron density enhanced by a factor of 10;

- A stronger depletion effect is expected for individual CMZ clouds, whose column densities are substantially larger than $N_{\text{H}_2}^{\text{CMZ}}$. For example, the expected depletion magnitude is a factor of ~ 5 higher for the central region of Sgr B2 (see Figure 3), where the column can exceed $N_{\text{H}_2}^{\text{CMZ}}$ by 1–2 orders of magnitude (see Protheroe et al. 2008). However, the radio emission from the Sgr B2 region is evidently dominated by the thermal component at all observed frequencies (see Figure 2), and therefore new observations at lower frequencies are needed to verify the depletion effect.

We would like to thank an anonymous referee for constructive and stimulating suggestions. The authors are grateful to Farhad Yusef-Zadeh for critical reading of the manuscript and useful comments, and to Roland Crocker for discussions. The work is supported by Russian Science Foundation via the Project 20-12-00047.

APPENDIX

CR FLUX VELOCITY AT THE EDGE IN DENSE CLOUD

To solve the problem of CR depletion self-consistently, one needs to evaluate the flux velocities $u_{p,e}$ of CR protons and electrons entering dense clouds with energies in a range from several hundreds of MeV to dozens of GeV. For these energies, the main mechanism of energy loss is bremsstrahlung for electrons, and pion production in nuclear collisions for protons. Both process can well be treated as catastrophic, since CR particles lose a significant fraction of their energy in each collision.

In the absence of scattering, CRs propagate along the magnetic field lines. Their spectrum is then described by the following equation:

$$v\mu \frac{\partial f}{\partial z} + \frac{f}{\tau} = 0, \quad (1)$$

with the boundary condition $f(0, p, \mu) = f_0(p, \mu)$. Here, μ is the pitch angle and $\tau^{-1} = v\sigma_{\text{loss}}n_{\text{H}_2}$ is the collision rate with H_2 molecules, determined by the cross section σ_{loss} for the relevant catastrophic loss mechanism (bremsstrahlung or pion production). If the CR spectrum at the cloud boundaries is isotropic, we have $f_0(p) = f^{(c)}(p)/2$. The resulting solution is

$$f(p, z, \mu) = f_0(p) \exp(-\sigma_{\text{loss}}n_{\text{H}_2}z/\mu), \quad (2)$$

and the flux velocity at the boundaries can be estimated as

$$u = \frac{1}{2} \int_0^1 v\mu \, d\mu - \frac{1}{2} \int_0^1 v\mu \exp(-\sigma_{\text{loss}}N_{\text{H}_2}/\mu) \, d\mu, \quad (3)$$

where $N_{\text{H}_2} = n_{\text{H}_2}L$ is the column density of a cloud of size L . For a typical case $\sigma_{\text{loss}}N_{\text{H}_2} \ll 1$, after a linear expansion of the second term we obtain

$$u \approx \frac{1}{2} v\sigma_{\text{loss}}N_{\text{H}_2}. \quad (4)$$

While CRs traveling inside dense clouds cannot normally trigger MHD waves because of a strong ion-neutral damping (see Kulsrud & Pearce 1969), the gas itself may be turbulent and thus the magnetic field lines can be strongly tangled. Propagation of CRs is then described as an “effective” diffusion (see e.g. the review of Hennebelle & Falgarone 2012). The energy of magnetic field fluctuations with $\delta B \gg B_0$ is concentrated near the correlation length, l_{corr} , and the effective diffusion coefficient of relativistic CRs is estimated as $D \sim cl_{\text{corr}}/3 \sim 10^{28} \text{ cm}^2 \text{ s}^{-1}$, assuming $l_{\text{corr}} \approx 0.5 \text{ pc}$ for molecular clouds with the size of several pc (Dogiel et al. 2015). We stress that this consideration does not require magnetic field to be perfectly frozen into the turbulent gas. In dense clouds, non-ideal MHD effects are dominated by a combination of magnetic diffusion due to finite conductivity and ion-neutral friction (Dogiel et

al. 1987; Istomin & Kiselev 2013), but turbulent gas motions generate significantly tangled magnetic field lines also under such conditions.

In a turbulent cloud with the effective diffusion coefficient D , the CR propagation is described by a simplified diffusion equation,

$$D \frac{\partial^2 f}{\partial z^2} - \frac{f}{\tau} = 0. \quad (5)$$

The boundary conditions are $f|_{z=0} = f|_{z=L} = f_0$ and the solution is

$$f(p, z) = f_0(p) \frac{\exp\left(\frac{L-z}{\sqrt{D\tau}}\right) + \exp\left(\frac{z}{\sqrt{D\tau}}\right)}{1 + \exp\left(\frac{L}{\sqrt{D\tau}}\right)}. \quad (6)$$

The flux velocity is

$$u = \frac{D}{f_0} \frac{\partial f}{\partial z} \Big|_{z=L} = \sqrt{\frac{D}{\tau}} \tanh\left(\frac{L}{2\sqrt{D\tau}}\right) \approx \frac{1}{2} v \sigma_{\text{loss}} N_{\text{H}_2}, \quad (7)$$

where the last (approximate) equality requires the condition $\sigma_{\text{loss}} N_{\text{H}_2} \ll l_{\text{corr}}/L$ to be satisfied. In the opposite

limit, the velocity approaches the value of

$$u \approx v \sqrt{\frac{1}{3} \frac{l_{\text{corr}}}{L} \sigma_{\text{loss}} N_{\text{H}_2}}, \quad (8)$$

where we substituted $D = vl_{\text{corr}}/3$. We conclude that u is not affected by the presence of turbulence in “thin” clouds (where the flux of CRs entering a cloud from one side is practically compensated by the opposite flux, arriving from the other side). On the other hand, for sufficiently large N_{H_2} or/and small l_{corr}/L , the flux velocity is smaller if a cloud is turbulent (since the diffusive propagation naturally suppresses the entering flux, while the compensation due to the opposite side is strongly attenuated). It is noteworthy that Equation (7) would also describe an (unlikely) situation if MHD fluctuations, leading to CR scattering, were present in a cloud: in this case the CR propagation is characterized by a certain (momentum-dependant) diffusion coefficient, and hence the above analysis remains applicable.

We use the bremsstrahlung cross section from Blumenthal & Gould (1970) and the pion production cross section from Aharonian & Atoyan (1996) to estimate the flux velocity of electrons and protons, respectively. In both cases, the condition $\sigma_{\text{loss}} N_{\text{H}_2} \ll 1$ is well satisfied for column densities below $\sim 10^{25} \text{ cm}^{-2}$. Therefore, unless l_{corr}/L is too small, Equations (4) and (7) yield the same expression for u , irrespective of whether the cloud is quiescent or turbulent. Furthermore, since the cross sections only weakly depend on the energy of relativistic CRs, we conclude that the flux velocities can be considered as constant.

REFERENCES

- Acerro, F., Ackermann, M., Ajello, M. et al. 2016, ApJS, 223, 26
- Aharonian, F. A., & Atoyan, A. M. 1996, A&A, 309, 917
- Bischoff, D., Potgieter, M. S., & Aslam, O. P. M. 2019, ApJ, 878, 59
- Blumenthal, G. R., & Gould, R. J. 1970, RvMP, 42, 237
- Crocker, R. M., Jones, D. I., Melia, F., Ott, J., & Protheroe, R. J. 2010, Natur, 463, 65
- De Angelis, A., Tatischeff, V., Argan, A. et al. 2021, arXiv: 2102.02460
- de Boer, W., Bosse, L., Gebauer, I., Neumann, A., & Biermann, P. L. 2017, PhRvD, 96, id.043012
- Dogiel, V. A., Gurevich, A. V., Istomin, Ia. N., & Zybin, K. P. 1987, MNRAS, 228, 843
- Dogiel, V. A., Chernyshov, D. O., Kiselev, A. M. et al. 2015, ApJ, 809, 48
- Dogiel, V. A., Chernyshov, D. O., Ivlev, A. V. et al. 2018, ApJ, 868, 114
- Ferrière, K., Gillard, W., & Jean, P. 2007, A&A, 467, 611
- Ferrière, K. 2009, A&A, 505, 1183
- Ginsburg, A., Henkel, C., Ao, Y. et al. 2016, A&A, 586, A50
- Ginzburg, V. L., & Syrovatskii, S. I. 1965, ARA&A, 3, 297
- Hennebelle, P., & Falgarone, E. 2012, A&ARv, 20, 55
- Hüttemeister, S., Wilson, T. L., Mauersberger, R., et al. 1995, A&A, 294, 667
- Indriolo, N., & McCall, B. J. 2012, ApJ, 745, 91
- Istomin, Ya. N., & Kiselev, A. M. 2013, MNRAS, 436, 2774
- Ivlev, A. V., Padovani, M., Galli, D., & Caselli, P. 2015, ApJ, 812, 135
- Ivlev, A. V., Dogiel, V. A., Chernyshov, D. O. et al. 2018, ApJ, 855, 23
- Jones, D. I., Protheroe, R. J., & Crocker, R. M. 2008, PASA, 25, 161
- Jones, D. I., Crocker, R. M., & Ott, J. 2011, AJ, 141, 82
- Jones, D. I. 2014, ApJL, 792, 14
- Kulsrud, R., & Pearce, W. 1969, ApJ, 156, 445
- Launhardt, R., Zylka, R., & Mezger, P. G. 2002, A&A, 384, 112

- McEnery, J. et al. (AMEGO Team) 2019, Bulletin of the American Astronomical Society, 51, 245
- Meng, F., Sánchez-Monge, Á., Schilke, P. et al. 2019, A&A, 630, A73
- Mills, E. A. C. 2017, arXiv:1705.05332
- Mills, E. A. C., Ginsburg, A., Immer, K. et al. 2018, ApJ, 868, 7
- Oka, T., Geballe, Th. R., Goto, M. et al. 2005, ApJ, 632, 882
- Oka, T., Geballe, T. R., Goto, M. et al. 2019, ApJ, 883, 54
- Owen, E. R., On, A. Y. L., Lai, S.-P., & Wu, K. 2021, ApJ, 913, 52
- Protheroe, R. J., Ott, J., Ekers, R. D. et al. 2008, MNRAS, 390, 683
- Riquelme, D., Bronfman, L., Mauersberger, R. et al. 2018, A&A, 610, A43
- Schönfelder, V., Aarts, H. J. M., Bennett, K. et al. 1993, A&AS, 97, 27
- Strong, A. W., Bennett, K., Bloemen, H. et al. 1996, A&AS, 120C, 381
- Schmiedeke, A., Schilke, P., Möller, Th. et al. 2016, A&A, 588, A143
- Tibaldo, L., Gaggero, D., & Martin, P. 2021, Univ, 7, 141
- Yusef-Zadeh, F., Wardle, M., & Roy, S. 2007, ApJ, 665, L123
- Yusef-Zadeh, F., Hewitt, J. W., Wardle, M. et al. 2013, ApJ, 762, 33
- Yusef-Zadeh, F., Cotton, W., Wardle, M. et al. 2016, ApJ, 819, L35